

Computational material modeling of masonry walls strengthened with fiber reinforced polymers

H. Orhun Köksal^{1a}, Oktay Jafarov^{2b}, Bilge Doran^{*3}, Selen Aktan^{1c} and Cengiz Karakoç^{4d}

¹Department of Civil Engineering, Çanakkale 18 Mart University, 17100 Çanakkale, Turkey

²Khazar University, Neftchilar Campus, AZ1096 Baku, Azerbaijan

³Department of Civil Engineering, Yıldız Technical University, 34220 Esenler, İstanbul, Turkey

⁴Department of Civil Engineering, Boğaziçi University, 34342 Bebek, İstanbul, Turkey

(Received February 20, 2013, Revised November 2, 2013, Accepted November 9, 2013)

Abstract. This paper aims to develop a practical approach to modeling of fiber reinforced polymers (FRP) strengthened masonry panels. The main objective is to provide suitable relations for the material characterization of the masonry constituents so that the finite element applications of elasto-plastic theory achieves a close fit to the experimental load-displacement diagrams of the walls subjected to in-plane shear and compression. Two relations proposed for masonry columns confined with FRP are adjusted for the cohesion and the internal friction angle of both units and mortar. Relating the mechanical parameters to the uniaxial compression strength and the hydrostatic pressure acting over the wall surface, the effects of major and intermediate principal stresses σ_1 and σ_2 on the yielding and the shape of the deviatoric section are then reflected into the analyses. Performing nonlinear finite element analyses (NLFEA) for the three walls tested in two different studies, their stress-strain response and failure modes are eventually evaluated through the comparisons with the experimental behavior.

Keywords: masonry wall; fiber reinforced polymer; cohesion; internal friction; elasto-plastic analysis; finite element

1. Introduction

From early history to modern times, masonry has been used for such a wide range of construction starting from ordinary walls to temples, palaces, defensive walls and city gates. Masonry structures are mostly located in many earthquake-prone regions and countries including Mediterranean area, India, the Middle East, Southeast Asia and Latin America. Unreinforced masonry (URM) buildings, which show little ductility, have consistently exhibited poor performance during past earthquakes and consequently unavoidable earthquake damages on these

*Corresponding author, Associate Professor, E-mail: doranbilge@gmail.com, doran@yildiz.edu.tr

^aProfessor, E-mail: hokksal@comu.edu.tr

^bCivil Engineer, E-mail: oktaycafer@gmail.com

^cResearch Assistant, E-mail: aktanselen@yahoo.com

^dProfessor, E-mail: karakoc@boun.edu.tr

structures led to a significant loss of world historical and cultural heritage. Therefore, the interest in seismic retrofitting of masonry structures has led to the development of specific engineering techniques and strategies in the last two decades. As one of the most popular retrofit techniques for seismic improvement of URM structures, rehabilitation of URM shear walls using FRP composites enhances their strength, flexibility and ductility under earthquake loading. The scope of the present study is confined to the finite element analysis (FEA) of URM walls strengthened with FRP composites by adopting an elasto-plastic approach proposed for the assessment of FRP-confined masonry columns under uniaxial compression (Köksal *et al.* 2012).

Several researchers have dealt with the finite element modeling of masonry in the last three decades. First studies (Hamid and Chukwunenye 1986, Cheema and Klingner 1986, Khalil *et al.* 1987, Ganesan and Ramamurthy 1992, Ramamurthy 1995, Sayed-Ahmed and Shrive 1996, Köksal *et al.* 2004, Köksal *et al.* 2005) are in the field of masonry prism testing and finite element modeling under compression in order to explain the stress distributions and the failure modes. Three-dimensional linear elastic finite element analyses of hollow block and grouted masonry prisms are initially carried out to predict their load carrying capacities in the absence of a reliable constitutive model to represent the complex behavior of masonry. Thereafter, Sayed-Ahmed and Shrive (1996) carried out a nonlinear three-dimensional FEA of 3-course block masonry prisms adopting Drucker-Prager (DP) yield criterion for prism behavior. The analysis of masonry structures has been actually based very much on the modeling approaches proposed in concrete and rock mechanics (Shing *et al.* 1992). Proceeding in a similar way with that used for the reinforced concrete (RC) members (Köksal and Karakoç 1999, Köksal and Arslan 2004), Köksal *et al.* (2004, 2005) employed a general-purpose finite element program LUSAS for modeling the unreinforced and reinforced masonry prisms and columns activating both the elasto-plastic and isotropic damage models to reflect the nonlinear behavior of the blocks, grout and mortar joints. Köksal *et al.* (2004, 2005) proposed a new model to achieve a close quantitative reproduction of the experimental results. Therefore, their first objective was to provide analytical relations for the suitable material parameters closely fit the load-displacement diagrams taking the large scatter in test results into account. Köksal *et al.* (2012) extended this approach to elasto-plastic modeling of FRP-confined masonry columns.

Researchers related to FE modeling of masonry walls subjected to compression and shear have initially taken similar steps in the modeling process for masonry prisms and columns under concentric loading. Masonry walls were assumed as isotropic and elastic ignoring the influence of mortar joints acting as planes of weakness. The fact that a complete constitutive model should reflect the inelastic material properties of the units and mortar, and a failure criterion describing the conditions for failure under combined compression-tension necessitated more detailed analytical studies (Dhanasekar 1984) and experimental investigations (Ganz and Thurlimann 1983). Meanwhile, Lourenco (1996) has been recognized for his important contribution to the FEA of masonry walls classifying the modeling strategies as detailed micro, simplified micro and macro-modeling. A micro model should include several material parameters such as elasticity modulus, Poisson's ratio, cohesion, internal friction angle, compressive and tensile strength for the representation of units and mortar. Moreover, the composite unit/mortar interface model recommended by Lourenco (1996) requires additional material parameters for the description of the interface behavior, e.g., tensile strength, cohesion, internal friction angle, compressive strength, tensile fracture energy, shear fracture energy and dilatancy angle. However, the great number of the influencing factors, such as difficulties in determining the mechanical properties of the construction materials due to the unknown construction period, the variety of construction

techniques, joint width and arrangement of bed and head joints, make the simulation of masonry wall behavior extremely difficult (Tzamtzis and Asteris 2003). All these uncertainties lead to a situation where the experimental results are more precise than their theoretical counterparts in the masonry design. Lourenco (1996) clearly stated that suitable relations for this large number of material parameters necessary to characterize his model were not proposed to recommend in his own theoretical study. In the same study, Lourenco (1996) acknowledged that the close prediction for the experimental load-displacement diagram could be possible in the application of the theoretical model if the shear properties were reduced 30 %, the compressive strength 20 % and the compressive fracture energy was multiplied by three. Furthermore, Milani *et al.* (2010) introduced additional material parameters into the FE analysis of the FRP-confined masonry indicating that the delamination is the most critical parameter to account for the determination of the ultimate displacement. From the engineering point of view, there is considerable limitation in the applicability of these sophisticated models (Chaimoon and Attard 2007, Giambanco *et al.* 2001, Lourenco and Rots 1997, Formica *et al.* 2002, Milani 2010, Grande *et al.* 2008) to FE analysis of masonry walls unless rational relations for the material parameters necessary to explain the models are provided.

This paper deals with the implementation of the plasticity theory to FRP-strengthened masonry walls under vertical and lateral loads by considering the constitutive behavior of masonry units, mortar and FRP composite material separately. Köksal *et al.* (2012) considered FRP-confined masonry columns as pressure-dependent material structures based on DP criterion. A DP type yield criterion is also employed relating the cohesion and the internal friction angle of both the masonry unit and mortar to their uniaxial compressive strength by extending the previous approach to the FRP-strengthened masonry walls. For this purpose, an extensive parametric study is performed in order to explain the mechanical properties of masonry units and mortar with only one single parameter, i.e., their uniaxial compressive strength (Jafarov 2012). Three masonry walls from two different studies (Stratford *et al.* 2004 and Capozucca 2011) which are unreinforced, single-sided strengthened with glass-fiber reinforced polymer (GFRP) and strengthened by carbon fiber reinforced polymers (CFRP) strips on one side respectively. These three walls are successively modeled using FEA method with the proposed approach in LUSAS software.

2. Material modeling

In order to reach a comprehensive understanding of masonry behavior, a number of experimental and analytical studies have been conducted on the behavior of masonry shear walls as the main structural component of masonry structures (Krstevska *et al.* 2007, Mele *et al.* 2003, Chaimoon and Attard 2007, Formica *et al.* 2002, Berto *et al.* 2002, Tasnimi and Farzin 2006, Mohebkah *et al.* 2008, Popohn *et al.* 2008). Proposed theoretical models for implementation to FE analysis of masonry generally require a large number of material parameters that are difficult to measure easily and reliably. For this reason, several attempts have been made to express the stress-strain relationships of the masonry and its constituents using different modeling techniques such as micro-modeling, homogenization approach and macro-modeling. The common approach in these studies is to treat masonry as a continuous medium or an equivalent continuous medium with the exception of detailed micro-modeling. Detailed micro-modeling should describe the masonry, mortar and the interaction behavior between them (Buhan and Felice 1997, Milani *et al.* 2006, Milani 2010, Brasile *et al.* 2010). Köksal *et al.* (2004, 2005, 2012) have performed FE analysis of

masonry prisms and columns strengthened with FRP describing the constitutive behavior of the unit, mortar and FRP separately. The similar approach has been adopted for the FE modeling of masonry shear walls while making the assumption that the material description of the mortar includes the effect of the unit-mortar interface behavior. Since the most common test performed on concrete-like brittle materials is for the measurement of its uniaxial compressive strength, it seems reasonable that the mechanical properties of masonry constituents can be assumed to be related to their compressive strengths. The authors have been adopted this strategy in the elasto-plastic analyses of RC elements, masonry prisms and columns successively (Köksal *et al.* 2009, Doran *et al.* 2009, Köksal *et al.* 2012).

2.1 Elasticity modulus of masonry constituents

The elasticity modulus of masonry is the most important mechanical parameter in FE analysis. The modulus of elasticity of masonry (E_m) can be determined by uniaxial compression tests. The failure mechanism and load-displacement behavior of masonry are strongly affected by the difference of elasticity modulus between unit and mortar (Mohamad *et al.* 2005, Jafarov 2012). The units have an imperious effect on the elasticity modulus of the masonry if the mortar is weaker than the units which is the most common case in the experiments. When it is not possible to test the masonry, approximate relations can be used for the determination of the modulus of elasticity. In detailed micro-modeling, elastic moduli of units and mortar are required for NLFEA of the masonry walls. If the masonry units are bricks, the following relation can be used for E_{br} :

$$E_{br} = (300\sim 700) f_{br} \quad (1)$$

where E_{br} and f_{br} are the elasticity modulus and compressive strength of bricks respectively. And if the concrete blocks or stone are used, the equation will be in the following form:

$$E_{bl} = 1000 f_{bl} \quad (2)$$

where E_{bl} and f_{bl} are the elasticity modulus and compressive strength of the blocks respectively. Since mortar is a softer and more ductile material, its elasticity modulus can be obtained from:

$$E_{mr} = 200 f_{mr} \quad (3)$$

where E_{mr} and f_{mr} are the elasticity modulus and compressive strength of the mortar respectively (Kaushnik *et al.* 2007, Jafarov 2012).

2.2 Elastoplastic modeling of masonry

Multi-axial stress states generally defines the behavior of the structures such as masonry walls, RC panels, confined columns or elements loaded over a specified limited area. The basic plastic models, i.e., Mohr-Coulomb (MC) and DP are widely adopted in constitutive modeling of frictional materials, like concretes, soils and rocks when describing the material behavior beyond the elastic range. Since material parameters of MC criterion are easily obtained from standard tests and are logical from the physical point of view, MC criterion is the most common used criterion in geotechnical and structural engineering. MC criterion in three-dimensional stress space can be expressed as:

$$f(\xi, \rho, \theta) = \sqrt{2}\xi \sin\Phi + \sqrt{3}\rho \sin\left(\theta + \frac{\pi}{3}\right) + \rho \cos\left(\theta + \frac{\pi}{3}\right) \sin\Phi - \sqrt{6}c \cos\Phi = 0$$

$$\text{for } 0 \leq \theta \leq \frac{\pi}{3} \tag{4}$$

where $\xi = I_1/\sqrt{3}$ and $\rho = \sqrt{2}J_2$. I_1 and J_2 are the first and second invariant of the stress and the deviatoric tensor respectively (Chen and Han 1988).

The invariants ξ and I_1 indicate the hydrostatic component of the current stress state. Because of the incompressibility of plastic deformations only ρ can contribute to the yielding for isotropic materials. In other words, ρ is the part of the stress that tends to change shape. Moreover, frictional materials typically show dependence on the invariant θ (Yu *et al.* 2010), which expresses itself as a dependence on the magnitude of the intermediate principal stress σ_2 with respect to the maximum and minimum principal stress values ($\sigma_1 > \sigma_2 > \sigma_3$) and affects the shape of the deviatoric section. For the deviatoric shape of the loading surface approaching a circular form as shown in Fig. 1, an increase in the ultimate load of a structural member is observed (Pivonka and William 2003). The behavior of civil engineering materials such as concrete, mortar, masonry units, rocks and soils exhibit a strong dependence on these three stress invariants. However, because of the smooth surface approximation to the six faceted MC yield function, DP criterion is conversely easy to implement and allows a fast computation of plastic behavior, even it is a drawback from the physical point of view (Maölino and Luong 2009, Köksal *et al.* 2012)

$$f(\xi, \rho) = \sqrt{6}\alpha\xi + \rho - \sqrt{2}k = 0 \tag{5}$$

where α and k are material constants.

As illustrated in Fig. 1, the actual deviatoric surface of pressure-dependent materials changes from the irregular hexagon to the circle under increasing hydrostatic pressures corresponding to a triaxial compressive stress state. One of the aims is to express the material parameters of DP criterion in terms of the cohesion and the internal friction angle in this study. Therefore, the surfaces of both DP and MC yield criteria are made to coincide along the compression meridian as shown in Fig. 2, and then the constants α and k are related to the constants c and ϕ by Chen and Han (1987):

$$\alpha = \frac{2\sin\phi}{\sqrt{3}(3-\sin\phi)} \quad , \quad k = \frac{6c \cos\phi}{\sqrt{3}(3-\sin\phi)} \tag{6}$$

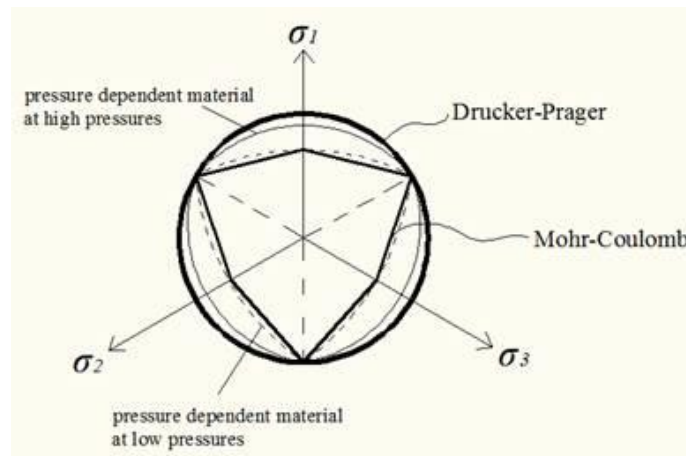


Fig. 1 Yield surfaces for pressure dependent materials in the deviatoric plane

In the previous works (Köksal *et al.* 2009) for NLFEA of RC columns confined with FRP, the ultimate strength values of the column predicted from a reliable criterion for concrete (Köksal 2006), have been used to determine the failure point in Haigh–Westergaard stress space. Making coincidence between that point within a specific range of hydrostatic pressure and the compressive meridian of DP criterion as illustrated in Fig. 3, the cohesion values can be determined while the internal friction angle is kept constant at 33° (Köksal *et al.* 2009, Doran *et al.* 2009). This procedure provides a better choice to improve the analytical results decreasing the overestimation possibility of DP criterion for NLFEA of frictional materials. As can be seen in Fig. 4, the lower limit for this approach is given as the stress levels of $\xi/f_{mu} \leq -0.58$.

A slightly different procedure is also adopted for the NLFEA of masonry columns strengthened with FRP (Köksal *et al.* 2012). Since the existence of major and intermediate principal stresses σ_1 and σ_2 will affect the yielding and the shape of the deviatoric section, the effect of FRP confinement should be include in the derivation of the material parameters. Due to the complexity of establishing a general failure surface in the principal stress space because of the lack of necessary experimental data, the mean stress $\sigma_m = I_1/3$ at the failure point is defined as a constant value which is corresponding to $(f_{mu} + 2f_l)/3$ at all stress levels where f_{mu} and f_l are the uniaxial compressive strength of the unit and the confining pressure exerted by FRP. In that study, new

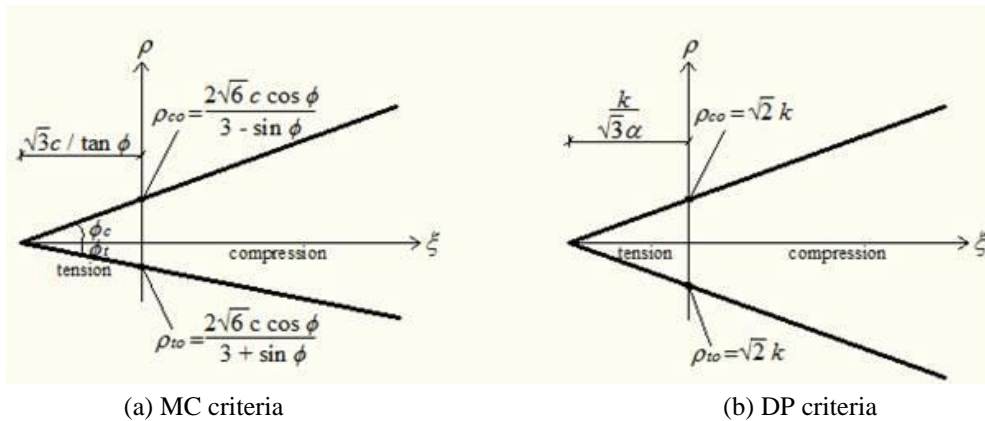


Fig. 2 Representation of compressive ($\theta=\pi/3$) and tensile ($\theta=0^\circ$) meridians

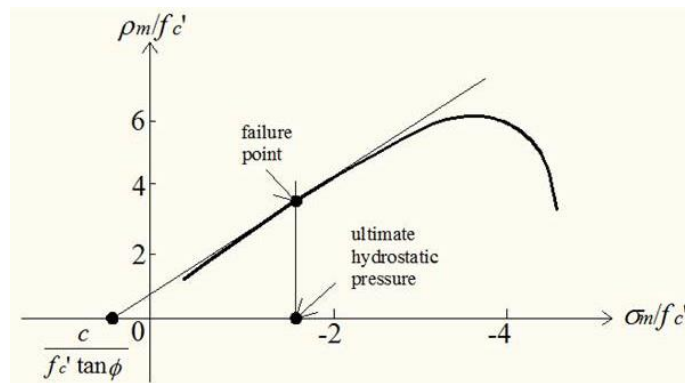


Fig. 3 Determination of the compressive meridian of DP criterion using the predicted failure point

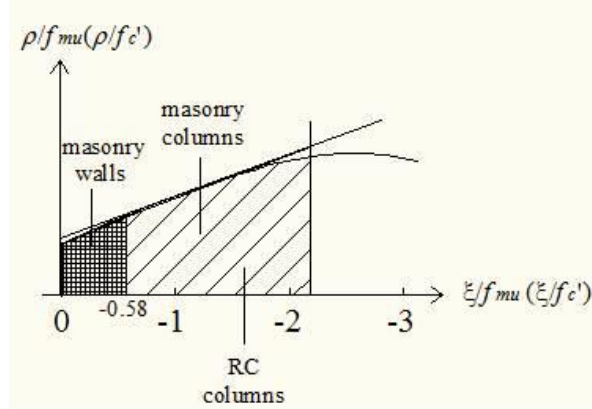


Fig. 4 Different hydrostatic pressure levels indicating possible failure points of masonry walls, RC columns and masonry columns

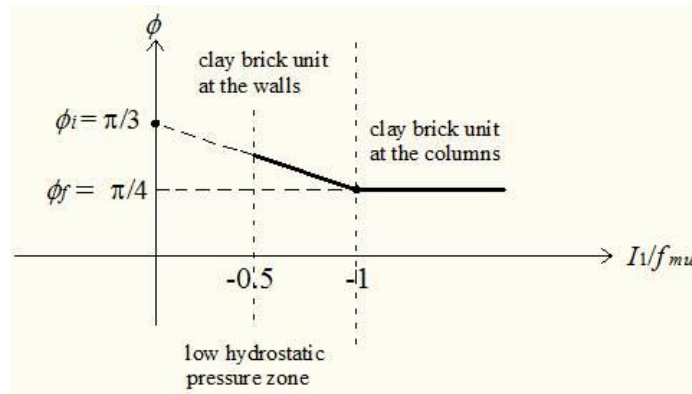


Fig. 5 Plotting of Eq. (8) for the internal friction angle of clay brick

relations have been proposed for the cohesion and the internal friction angle of the units to include the confinement stresses:

$$\frac{c_{mu}}{f_{mu}} = \frac{\tan \phi_{mu}}{3} \sqrt{\frac{|\sigma_m|}{f_{mu}}} \leq \frac{c_{mu}}{f_{mu}} \Big|_{\frac{|\sigma_m|}{f_{mu}}=1} \quad (7)$$

$$\phi_{mu} = \phi_i - 0.75 \frac{|\sigma_m|}{f_{mu}} \geq \phi_f = \phi_{mu} \Big|_{\frac{|\sigma_m|}{f_{mu}}=1} \quad (8)$$

where ϕ_i and ϕ_f are initial and final angle of internal friction in radians respectively. ϕ_i can be nearly equal to $\pi/3$ for brick and $\pi/4$ for concrete. Applying the boundary condition in Eq. (8), ϕ_f is approximately $\pi/4$ for brick and between $\pi/5$ and $\pi/6$ for concrete. For high hydrostatic pressures ($0 < \sigma_m/f_{mu} \leq 1$), internal friction angle can be taken as a constant value, i.e., 30° - 35° for concrete and nearly 45° for clay brick as illustrated in Fig. 5.

Since much lower pressures exist on masonry walls and their constituents, material parameters have been calibrated to best reconcile the experimental data of several walls. In the wall tests, as the axial load level is less than the ultimate uniaxial strength, the mean stress can be taken as a

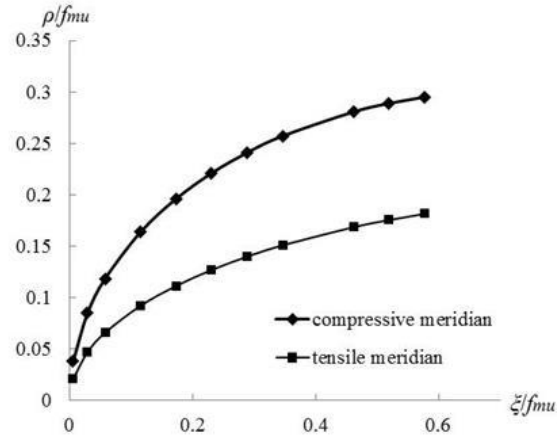


Fig. 6 Modified form of the compressive and tensile meridians of MC criterion using Eqs. (7) and (8)

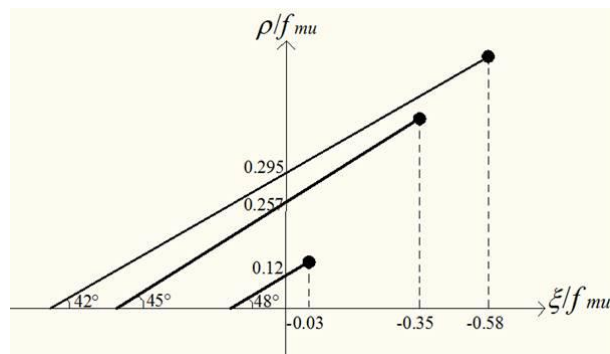


Fig. 7 Predictions for some failure points on the compression meridians of DP criterion

constant value corresponding to $(p+2f_i)/3$ at all stress levels. In here, p and f_i are the vertical pre-compression of the wall and the confining pressure of FRP material. The validity of Eqs. (7)-(8) is finally verified by numerical simulations of the walls subjected to the pressures in the range of $\xi/f_{mu} \leq -0.58$ throughout this study and plots of compressive and tensile meridians are given in Fig. 6. While plotting the meridians, values of cohesion and internal friction angles obtained from Eqs. (7)-(8) are replaced into Eq. (4). Expressing the cohesion and internal friction angles by changing hydrostatic pressure modifies the straight line form of MC criterion into a curved one. Failure and yield surfaces of DP criterion are then defined by the compressive meridians of MC criterion. For $\sigma_m/f_{mu} \geq -1$ ($\xi/f_{mu} \leq -0.58$), predictions for some failure points on the compression meridians of DP criterion are plotted in Fig. 7.

While simulating the behavior of masonry walls under shear-compression fracture, as can be seen in Fig. 8(a) if shear loading is omitted, the stress state will be the uniaxial compression. Therefore, the elasto-plastic behavior of the units and the mortar can be described by a DP criterion represented by the compressive meridian of MC criterion reducing the differences between the finite element application of two criteria for the range of $\xi/f_{mu} \leq -0.58$. However, for increasing shear loading in Fig. 8(b), the stress state of the units and the mortar at failure will approach to the tensile meridian of MC criterion. The use of the compressive meridian obviously

causes some overestimation for the failure load for this case. In order to lessen this overestimation, an ending point definition for the termination of NLFEA is developed in this study (Jafarov 2012). The ending point for the analysis can be determined defining the discontinuity surface between two units along the thickness of the mortar as illustrated in Fig. 9. The maximum tensile strain can then be determined from the case of that a complete opening will occur along the mortar thickness between two units as:

$$\varepsilon_{max} = h_{mr} / (2h_{br} + h_{mr}) \tag{9}$$

where h_{mr} is the mortar thickness and h_{br} is the height of the unit.

Mortar generally governs the nonlinear behavior of masonry and has an influence in the axial strain of masonry prism and also on the shear response of the masonry walls (Haach *et al.* 2010, Jafarov 2012). Therefore, any theoretical model should account for the nonlinear response of both the mortar and the unit-mortar interface to predict the inelastic behavior of masonry (Mohamad *et al.* 2005, Marcari *et al.* 2007). In this study, the mechanical parameters of mortar, e.g., cohesion c_{mr} and internal friction angle ϕ_{mr} , are adjusted to reflect the unit-mortar interface response as preferred in the modeling of masonry prisms and columns previously (Köksal *et al.* 2004, Köksal *et al.* 2012):

$$c_{mr} = 1.55^3 \sqrt{f_{mr}} \tag{10}$$

$$\phi_{mr} = 1.519 f_{mr} \text{ (MPa)} \tag{11}$$

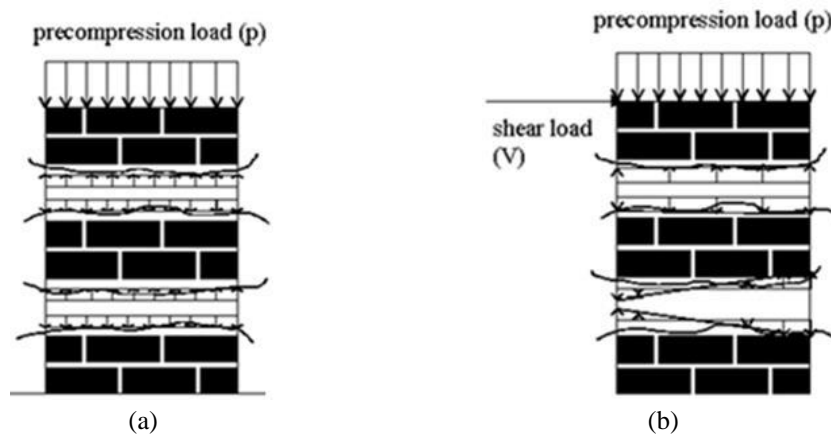


Fig. 8 Masonry walls under (a) uniaxial compression (b) shear compression

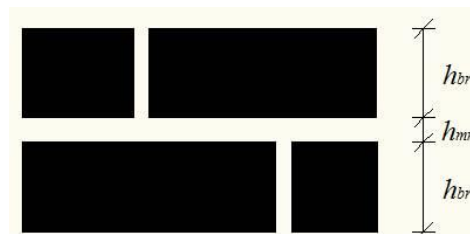


Fig. 9 Assumption for the discontinuity surface between two units along the thickness of the mortar resulting failure of the wall

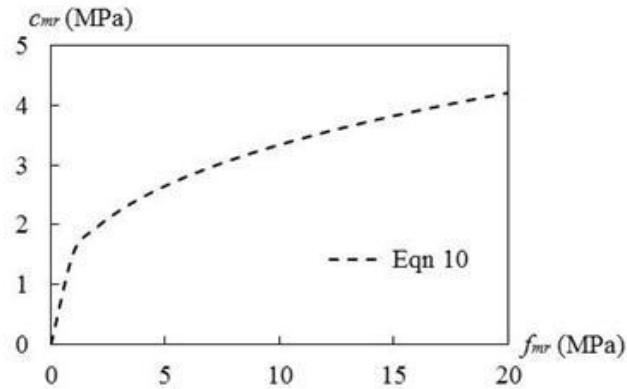


Fig. 10 Plotting of Eq. (10) for estimating cohesion of mortar

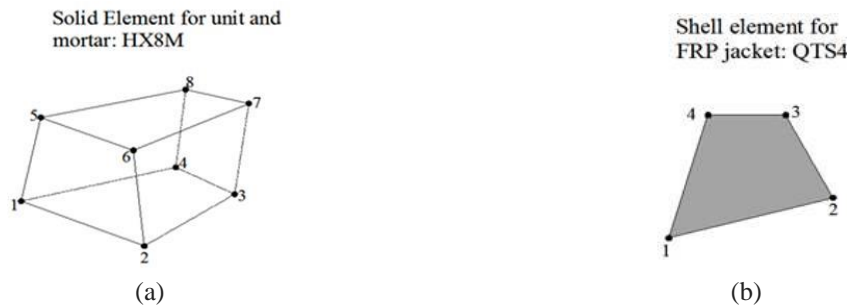


Fig. 11 (a) Eight-noded hexahedral element for units and mortar (b) four-noded thick shell element for FRP jacket

In a previous study (Köksal *et al.* 2004), a linear relation was proposed between the cohesion and the uniaxial compression strength of mortar f_{mr} . While developing a relation for the mortar cohesion, taking the effect of the unit-mortar interface behavior into account, probably makes the cohesion more sensitive to the changes in its strength for the walls under shear-compression (Fig. 10). A perfect bond is accordingly assumed between masonry unit and mortar and a reliable and robust analysis can be achieved on the computational complexity of solution algorithms.

3. Finite element modeling and model verification

Three dimensional (3D) finite element models are used for masonry walls strengthened with FRP composites in LUSAS (Lusas 2011). Masonry constituents, i.e., brick and mortar, are assumed to be isotropic elasto-plastic obeying DP criterion. They are modeled separately with eight-noded hexahedral element (HX8M) which is a solid element with an incompatible strain field as illustrated in Fig. 11(a). FRP composites are modeled by four-noded thick shell element (QTS4) which has a thick and thin curved shell geometry including multiple branched junctions as in Fig. 11(b). Both the element formulations take account of membrane, shear and flexural deformations and capable of modeling inelastic phenomenon.

Table 1 Mechanical properties adopted for FE analyses

Reference	Experiment	Brick			Mortar		
		E_{mu} (MPa)	c_{mu} (MPa)	ϕ_{mu} (°)	E_{mr} (MPa)	c_{mr} (MPa)	ϕ_{mr} (°)
Stratford	Clay1 URM	18600	3.04	59.68	3250	3.45	16.71
Stratford	Clay 2 GFRP	18600	3.04	59.68	3250	3.45	16.71
Capozucca	HRM-C2	7000	2.33	59.37	150	2.21	4.41

Table 2 General characteristics of masonry walls and FRP confinement

Reference	Experiment	Precompression Load (MPa)	Wall Dimension (mm)	Brick Dimension (mm)	FRP	
					E_{FRP} (MPa)	t (mm)
Stratford	Clay 1 URM	1.38	1200×1200×60	228×65×60	-	-
Stratford	Clay 2 GFRP	1.38	1200×1200×60	228×65×60	73300	0.15
Capozucca	HRM-C2	1.5	840×633×50	100×17×50	240000	0.177

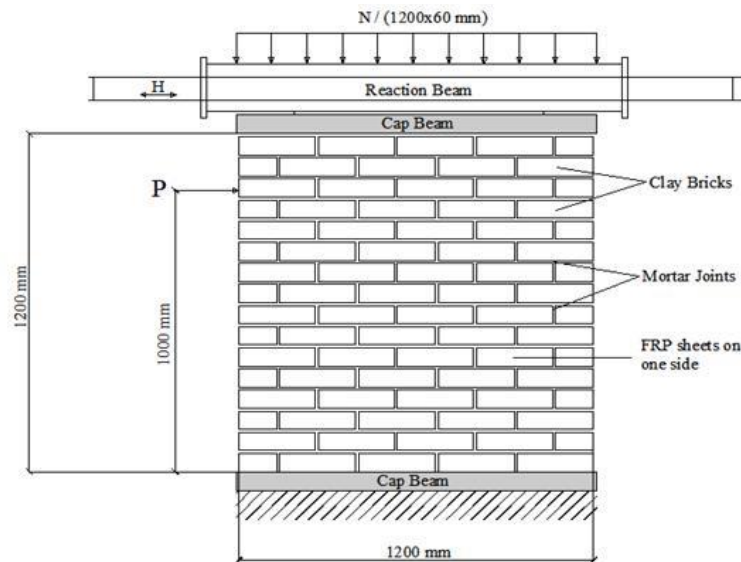


Fig. 12 Experimental setup of shear wall clay 2

Table 1 shows the material and geometrical properties for masonry walls with its FRP confinement evaluated in this study. All mechanical properties of the masonry constituents utilized in the analyses are also given in Table 2.

Stratford *et al.* (2004) tested six 1200×1200 mm masonry panels under a combination of vertical preloading, and in-plane horizontal shear loading. Both clay and concrete brick specimens were tested while one specimen of each material was left unreinforced and the other two panels were single-sided strengthened using GFRP. GFRP had equal amounts of fibers in the horizontal and vertical directions (parallel to the mortar joints) and fibers were oriented at 45° to the joints. As can be seen in Fig. 12, two connected hydraulic jacks (N) were placed on the wall while the shear load was applied to the wall by a horizontal hydraulic jack (P).

For the case of URM wall, the end point for the FEA is determined defining a discontinuity surface between two clay units along the thickness of the mortar. The maximum tensile strain

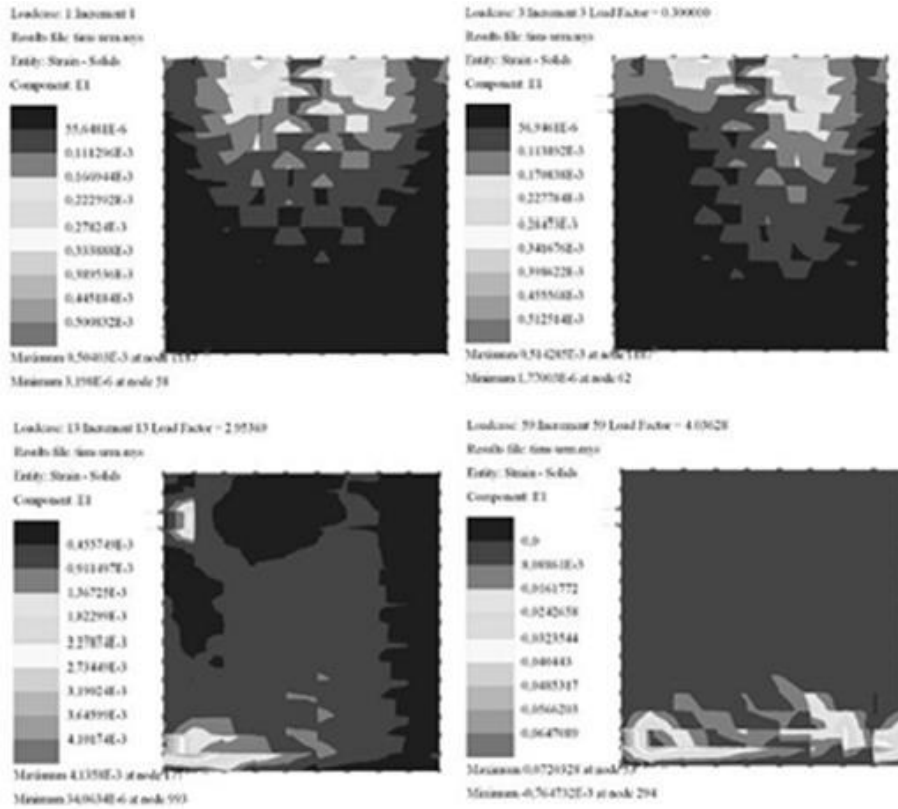


Fig. 13 Maximum strains along the wall height

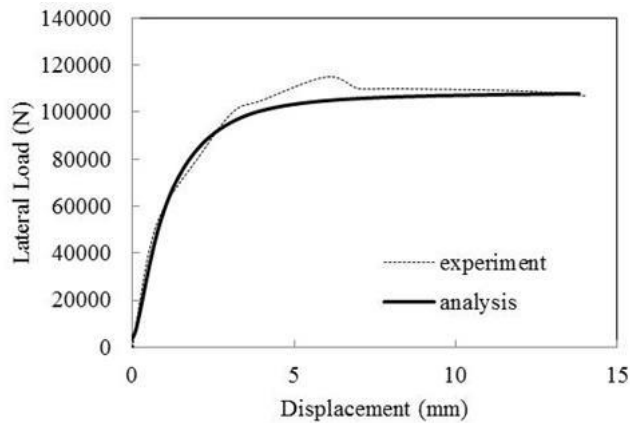


Fig. 14 Lateral load–displacement responses for clay 1

pointing out that a complete opening will occur along the mortar thickness between two units, can be found by dividing the mortar joint thickness 10 mm by two block heights plus the mortar thickness as $10/(2 \times 65 + 10) = 0.071$. This strain value can be called critical tensile strain. As the lateral load is increased, the effect of tensile deformations grows up along the toe of the wall and it

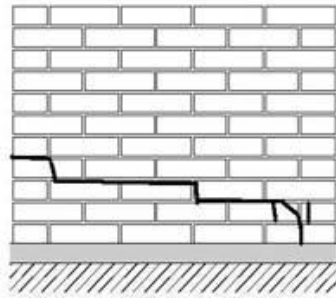


Fig. 15 Experimental crack pattern for clay 1

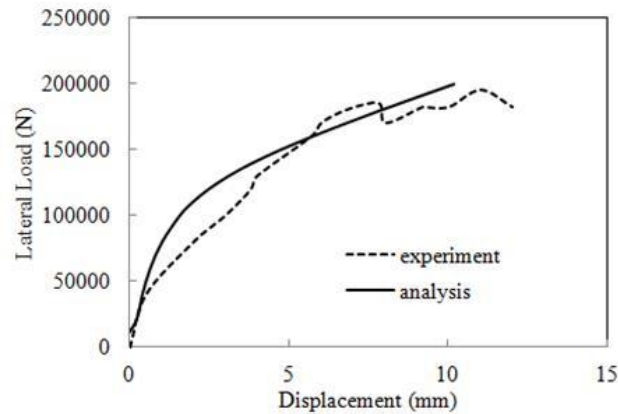


Fig. 16 Lateral load–displacement responses for strengthened clay 2

is easy to observe the critical tensile strain is observed at the toe of the wall from Fig. 13. If FEA ends when the ultimate tensile strain at the wall reaches the critical value, both simulation model and laboratory test results agreed very well as shown in Fig. 14.

As can be seen in Fig. 14, horizontal displacement at the failure is experimentally determined approximately as 14 mm. NLFEA gives a value of 13.81 mm from the use of the maximum tensile strain criterion for the wall. As can be seen in Figs. 13 and 15, the region of concentrated maximum tensile strain matches the location of experimental crack pattern on the wall.

Fig. 16 shows the stress-strain plots for strengthened wall clay 2. The load-displacement plot obtained from NLFEA is well agreed with the experimental data. As shown in Fig. 17, the analysis is terminated upon reaching the maximum tensile strain corresponding to the tensile strength of GFRP at a horizontal drift of 10.16 mm. This value is experimentally determined approximately as 12 mm.

In all experiments, except for the unreinforced clay specimen (clay 1), the strengthened masonry walls (clay 2) failed by rapid propagation of diagonal crack which followed the mortar joints as in Fig. 18(a). Crushing failure, which occurred when the compressive strength of the mortar was reached, cannot be occurred for these walls because of the mortar strength higher than 11 MPa. Shear failure, involving sliding along a slip plane either within the mortar or at the brick–mortar interface; is the main failure mode. The fracture pattern is well predicted through the concentration of the maximum tensile strains diagonally shown in Fig. 18(b).

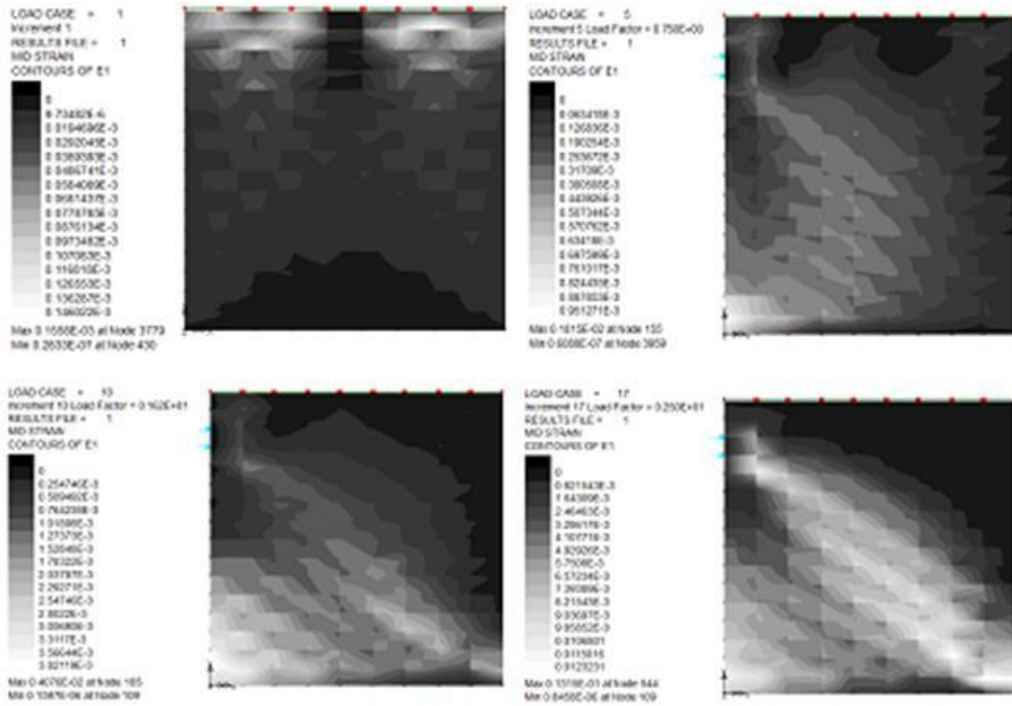


Fig. 17 Maximum strain distribution over GFRP surface

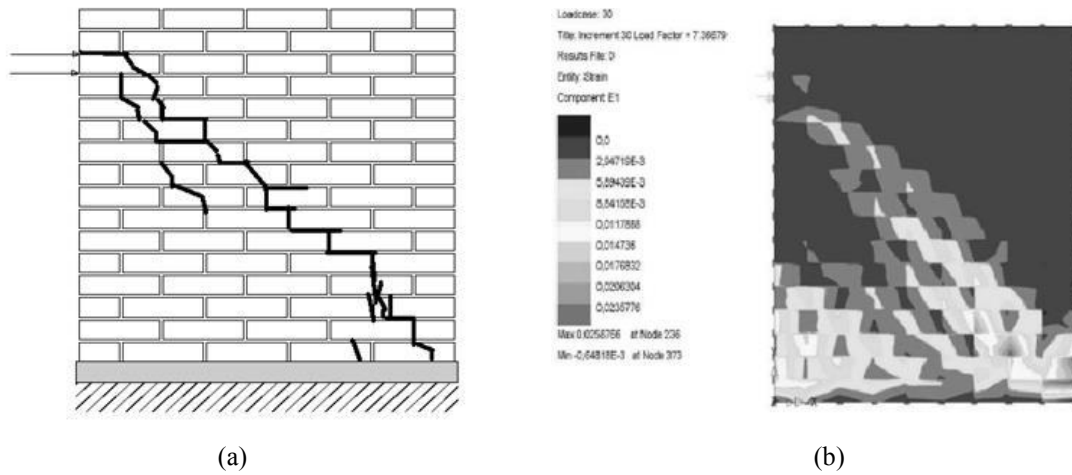


Fig. 18 (a) Schematic crack patterns in strengthened wall (clay 2), and (b) maximum tensile strains over unreinforced face in 3D FE model

Capozucca (2011) investigated the behavior of Historical Reinforced Masonry (HRM) walls strengthened by CFRP strips, experimentally. CFRP strips bonded to only one face of the specimen in horizontally and vertically. Strips of FRP, containing unidirectional fibers, can be bonded to the surface of the wall and arranged to provide an external truss action (Stratford *et al.* 2004). The

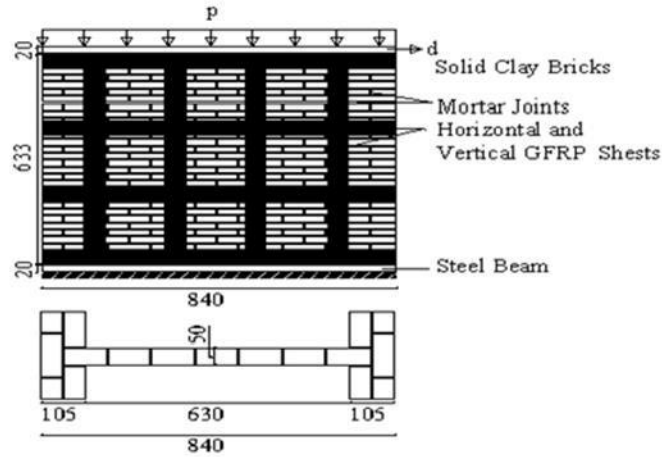


Fig. 19 Geometrical details of HRM C2 wall (Capozucca 2011)

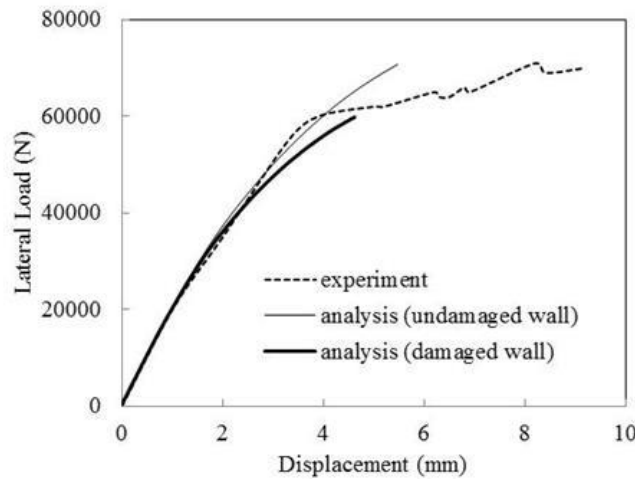


Fig. 20 Comparison of load–displacement responses for pre-damaged HRM C2 wall employing the ultimate tensile strain criterion of GFRP

strengthened wall was subjected to cyclic loading until failure. Specimens were built with clay bricks and mortar with thickness 4 mm. Flexural tensile strength of mortar was 0.80 MPa. A single-story HRM C2 wall was built using historic full clay bricks in scale one-third and tested in a special frame (Fig. 19). Besides, mechanical and geometrical properties of brick, mortar and CFRP strips are given here in Tables 1-2.

Initially, pre-compression load (1.50 MPa) was applied to the flanges and web by three jacks, kept constant, then horizontal force was applied measuring horizontal force until failure (Capozucca 2011). Wall C2 damaged by cyclic shear tests and then was strengthened by 50 mm wide carbon strips bonded to one side, parallel and normal to mortar joints. Mechanical parameters of CFRP strips are summarized in Table 2. Walls C1 and C2 were initially subjected, respectively, to five cyclic stages of horizontal force and seven cyclic stages before to bring the walls to failure by an ultimate stage with unidirectional horizontal force (Capozucca 2011). These are the possible

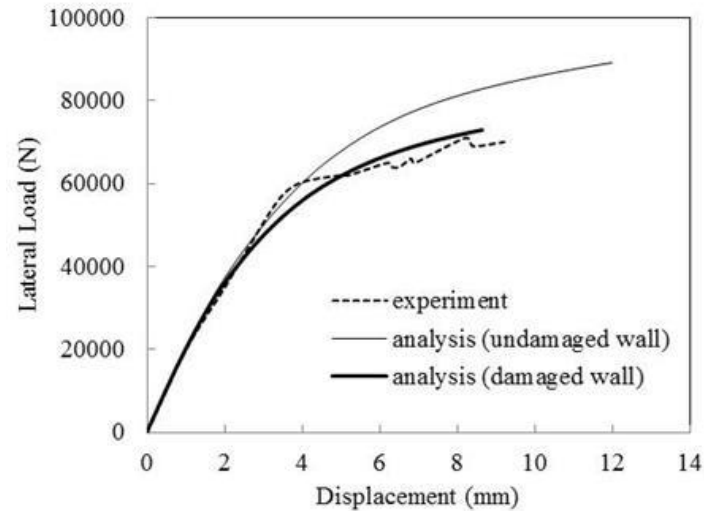


Fig. 21 Comparison of load–displacement responses for pre-damaged HRM C2 wall adopting the maximum tensile strain criterion of masonry

reasons for the stiffer behavior observed in Figs. 20–21. The critical tensile strain assumption for masonry is adopted for the stress-strain plots (Fig. 21), while the analysis is terminated by reaching the tensile strength of GFRP as in Fig. 20. Therefore, the material parameters for the masonry constituents of the pre-damaged walls should be somewhat lower than the recommended ones in Eqs. (7)–(10). The cohesion and internal friction angle values of the clay brick lowered by 35% and 15% respectively. Since the mortar has already defined by a very weak material, any reduction on its mechanical properties will not be reasonable. Another reason for the stiffer predictions can be the present approach does not consider the debonding phenomenon between the wall and FRP layer which affects the maximum lateral displacement of the wall particularly while reaching the ultimate load capacity (La Mendola *et al.* 2009).

Actually, presence of discontinuity surfaces with some specific values of separation affects the failure mechanisms and the level of FRP confinement in cracked and damaged walls. Therefore, the use of the critical tensile strain criterion instead of the ultimate tensile strength of FRP can be more reasonable for the analysis of pre-damaged walls.

4. Conclusions

This paper is primarily concerned with 3D elastic-plastic analysis under compression and shear, employing the DP yield criterion for URM and strengthened walls. The material parameters for brick and mortar are expressed in terms of the compressive strength of masonry throughout the analysis. In order to evaluate the accuracy of the proposed approach, the analytical results are compared with the experimental results of both unreinforced and strengthened masonry walls tested in two different experimental studies. Following conclusions are drawn:

- The analytical approach previously developed for the elasto-plastic analysis of masonry columns are extended to the masonry walls under shear-compression in this paper. Masonry units

and mortar are considered separately as isotropic and homogeneous materials. Since much lower pressures exist on masonry walls and their constituents, material parameters have been recalibrated to best reconcile the test data of several walls in the literature.

- Cohesion and internal friction values of the masonry units are expressed in terms of hydrostatic pressure at the failure and their uniaxial compressive strength. The relations of masonry constituents are recommended and are valid for $\xi/f_{mu} < 0.58$. The dependency of the material parameters of the frictional materials on the hydrostatic pressure is then reflected into the analysis directly.

- The material parameters of DP criterion are expressed in terms of the cohesion and the internal friction angle of MC criterion in this study. Therefore, the surfaces of both DP and MC yield criteria are made to coincide along the compression meridian.

- The use of the compressive meridian obviously causes some overestimation for the failure load for increasing shear loading. In order to reduce possible overestimation, a critical tensile strain is defined for the termination of NLFEA is developed in this study. It is possible to calculate the critical tensile strain by dividing the mortar thickness by two block heights plus the mortar thickness assuming that a complete opening will occur along the mortar thickness between two units.

- The lateral load-displacement plots obtained for NLFEA of URM wall tested by Stratford are in good agreement with the test results. The failure load and displacement are well predicted by the use of the critical tensile strain criterion.

- For strengthened wall clay 2, the load-displacement plot obtained from NLFEA is again well agreed with the experimental data. For this case, the analysis is terminated upon reaching the maximum tensile strength of GFRP.

- For the pre-damaged walls, the proposed approach can still be used as shown in the NLFEA of Capozucca's walls. However, the material properties of the unit and mortar should be lowered. Degree of the reduction on the mechanical properties clearly depends on the damage level of the wall. A future work has been planned for the mechanical representation of the repaired masonry walls with FRP jackets which were previously damaged under varied levels of load.

References

- Berto, L., Saetta, A., Scotta, R. and Vitaliani, R. (2002), "An orthotropic damage model for masonry structures", *Int. J. Numer. Meth. Eng.*, **55**(2), 127-157.
- Brasile, S., Casciaro, R. and Formica, G. (2010), "Finite element formulation for nonlinear analysis of masonry walls", *Comput. Struct.*, **88**(3-4), 135-143.
- Capozucca, R. (2011), "Experimental analysis of historic masonry walls reinforced by CFRP under in-plane cyclic loading", *Compos. Struct.*, **94**(1), 277-289.
- Chaimoon, K. and Attard, M.M. (2007), "Modeling of unreinforced masonry walls under shear and compression", *Eng. Struct.*, **29**(9), 2056-2068.
- Cheema, T.S. and Klingner, R.E. (1986), "Compressive strength of concrete masonry prisms", *J. Am. Concrete Ins.*, **83**(1), 88-97.
- Chen, W.F. and Lui, E.M. (1987), *Structural Stability: Theory and Implementation*, Elsevier, New York.
- Chen, W.F. and Han, D.J. (1988), *Plasticity for Structural Engineers*, Springer-Verlag, New York.
- DeBuhan, P. and DeFelice, G. (1997), "A homogenization approach to the ultimate strength of brick masonry", *J. Mech. Phys. Solid.*, **45**(7), 1085-1104.
- Dhanasekar, M., Page, A.W. and Kleeman, P.W. (1984), "A finite element model for the in-plane behavior

- of brick masonry”, *Proc. 9th Australasian Conference on Mechanisms of Structures*, 262-267.
- Doran, B., Köksal, H.O. and Turgay, T. (2009), “Nonlinear finite element modeling of rectangular/square concrete columns confined with FRP”, *Mater. Des.*, **30**(8), 3066-3075.
- Formica, G., Sansalone, V. and Casciaro, R. (2002), “A mixed solution strategy for the nonlinear analysis of brick masonry walls”, *Comput. Meth. Appl. Mech. Eng.*, **191**(51-52), 5847-5876.
- Ganesan, T. and Ramamurthy, K. (1992), “Behavior of concrete hollow-block masonry prisms under axial-compression”, *J. Struct. Eng.*, **118**(7), 1751-1769.
- Ganz, H.R. and Thurlimann, B. (1983), “Strength of brick walls under normal force and shear”, *Proc. 8th Int. Symp. On Load Bearing Brickwork*, London, U.K.
- Giambanco, G., Rizzo, S. and Spallino, R. (2001), “Numerical analysis of masonry structures via interface models”, *Comput. Meth. Appl. Mech. Eng.*, **190**(49-50), 6493-6511.
- Grande, E., Milani, G. and Sacco, E. (2008), “Modelling and analysis of FRP-strengthened masonry panels”, *Eng. Struct.*, **30**(7), 1842-1860.
- Haach, V.G., Vasconcelos, G. and Lourenco, P.B. (2010), “Influence of the geometry of units and filling of vertical joints in the compressive and tensile strength of masonry”, *Mater. Sci. Forum*, Special Issue, **636-637**, 1321-1328.
- Hamid, A.A. and Chukwunye, A.O. (1986), “Compression behavior of concrete masonry prisms”, *J. Struct. Eng.*, **112**(3), 605-613.
- Jafarov, O. (2012), “Lifli polimerle güçlendirilmiş yığma duvarların modellenmesi”, Ph.D. Thesis, Civil Engineering, Yıldız Technical University, Istanbul.
- Kaushik, H.B., Rai, D.C. and Jain, S.K. (2007), “Stress-strain characteristics of clay brick masonry under uniaxial compression”, *J. Mater. Civil Eng.*, **19**(9), 728-739.
- Khalil, M.R.A., Shrive, N.G. and Ameny, P. (1987), “3 dimensional stress-distribution in concrete masonry prisms and walls”, *Mag. Concrete Res.*, **39**(139), 73-82.
- Köksal, H.O. and Karakoç, C. (1999), “An isotropic damage model for concrete”, *Mater. Struct.*, **32**(222), 611-617.
- Köksal, H.O., Doran, B., Ozsoy, A.E. and Alacalı, S.N. (2004), “Nonlinear modeling of concentrically loaded reinforced blockwork masonry columns”, *Can. J. Civil Eng.*, **31**(6), 1012-1023.
- Köksal, H.O. and Arslan, G. (2004) “Damage analysis of RC beams without web reinforcement”, *Mag. Concrete Res.*, **56**(4), 231-241.
- Köksal, H.O., Karakoç, C. and Yıldırım, H. (2005), “Compression behavior and failure mechanisms of concrete masonry prisms”, *J. Mater. Civil Eng.*, **17**(1), 107-115.
- Köksal, H.O. (2006), “A failure criterion for RC members under triaxial compression”, *Struct. Eng. Mech.*, **24**(2), 137-154.
- Köksal, H.O., Doran, B. and Turgay, T. (2009), “A practical approach for modeling FRP wrapped concrete columns”, *Constr. Build. Mater.*, **23**(3), 1429-1437.
- Köksal, H.O., Aktan, S. and Kuruşçu, A.O. (2012), “Elasto-plastic finite element analysis of FRP-confined masonry columns”, *J. Compos. Construct.*, **16**(4), 407-417.
- Krstevska, L., Tashkov, Lj., Arun, G. and Aköz, F. (2007), “Evaluation of seismic behavior of historical monuments”, *SHH07 International Symposium on Studies on Historical Heritage Symposium Book*, Antalya, Turkey.
- La Mendola, L., Failla, A., Cucchiara, C. and Accardi, M. (2009), “Debonding phenomena in CFRP strengthened calcarenite masonry walls and vaults”, *Adv. Struct. Eng.*, **12**(5), 745-760.
- Lourenco, P.B. (1996), “Computational strategies for masonry structures”, Ph.D. Thesis, Civil Engineering and Geosciences, Delft University, Eindhoven, Netherland.
- Lourenco, P.B. and Rots, J.G. (1997), “Multisurface interface model for analysis of masonry structures”, *J. Eng. Mech.*, **123**(7), 660-668.
- LUSAS Finite Element System, Version 14.5-2 (2011), FEA Ltd, Surrey, UK.
- Maölino, S. and Luong, M.P. (2009), “Measuring discrepancies between coulomb and other geotechnical criteria: drucker-prager and matsuoaka-nakai”, *Proceedings of the 7th EUROMECH Solid Mechanics Conference*, Lisbon, Portugal, September.

- Marcari, G., Fabbrocino, G., Manfredi, G. and Prota, A. (2007), "Experimental and numerical evaluation of tuff masonry panels shear seismic capacity", *Proceedings of the 10th North American Masonry Conference*, St. Louis, USA.
- Mele, E., De Luca, A. and Giordano, A. (2003), "Modelling and analysis of a basilica under earthquake loading", *J. Cultur. Heritage*, **4**(4), 355-367.
- Milani, G., Lourenco, P.B. and Tralli, A. (2006), "Homogenised limit analysis of masonry walls, part I: failure surfaces", *Comput. Struct.*, **84**(3-4), 166-180.
- Milani, G. (2010), "3D FE limit analysis model for multi-layer masonry structures reinforced with FRP strips", *Int. J. Mech. Sci.*, **52**(6), 784-803.
- Milani, G., Milani, E. and Tralli, A. (2010), "Approximate limit analysis of full scale FRP-reinforced masonry buildings through a 3D homogenized FE package", *Compos. Struct.*, **92**(4), 918-935.
- Mohamad, G., Lourenco, P.B. and Roman, H.R. (2005), "Mechanical behavior assessment of concrete block masonry prisms under compression", *Int. Conf. on Concrete for Structures*, Coimbra, Portugal.
- Mohebkah, A., Tasnimi, A.A. and Moghadam, H.A. (2008), "Nonlinear analysis of masonry-infilled steel frames with openings using discrete element method", *J. Constr. Steel Res.*, **64**(12), 1463-1472.
- Pivonka, P. and Willam, K. (2003), "The effect of the third invariant in computational plasticity", *Eng. Comput.*, **20**(5/6), 741-753.
- Popehn, J.R.B., Schultz, A.E., Lu, M., Stolarski, H.K. and Ojard, N.C. (2008), "Influence of transverse loading on the stability of slender unreinforced masonry walls", *Eng. Struct.*, **30**(10), 2830-2839.
- Ramamurthy, K. (1995), "Behavior of grouted concrete hollow block masonry prisms", *Mag. Concrete Res.*, **47**(173), 345-354.
- Sayed Ahmed, E.Y. and Shrive, N.G. (1996), "Nonlinear finite-element model of hollow masonry", *J. Struct. Eng.*, **122**(6), 683-690.
- Shing, P.B., Lofti, H.R., Barzegarmehrabi, A. and Brunner, J. (1992), "Finite-element analysis of shear resistance of masonry wall panels with and without confining frames", *Proceedings of the Tenth World Conference on Earthquake Engineering*, **1-10**, 2581-2586.
- Stratford, T., Pascale, G., Manfroni, O. and Bonfiglioli, B. (2004), "Shear strengthening masonry panels with sheet glass-fiber reinforced polymer", *J. Compos. Constr.*, **8**(5), 434-443.
- Tasnimi, A.A. and Farzin, M. (2006), "Inelastic behavior of RC columns under cyclic loads, based on cohesion and internal friction angle of concrete", *Modar. Tech. Eng. J.*, ISSN, **23**, 29-40.
- Tzamtzis, A.D. and Asteris, P.G. (2003), "Finite element analysis of masonry structures: part I- review of previous work", *North American Masonry Conference*, Clemson, South Carolina, June.
- Yu, T., Teng, J.G., Wong, Y.L. and Dong, S.L. (2010), "Finite element modeling of confined concrete-I: drucker-prager type plasticity model", *Eng. Struct.*, **32**(3), 665-679.